Research article

Differential localization in cells of myosin II heavy chain kinases during cytokinesis and polarized migration

Wenchuan Liang[1], Lucila S Licate[2], Hans M Warrick[1], James A Spudich[1] and Thomas T Egelhoff*[2]

Address: [1]Department of Biochemistry, Stanford University School of Medicine, Stanford, CA 94305-5307, USA and [2]Department of Physiology and Biophysics, Case Western Reserve School of Medicine, Cleveland, OH 44106-4970, USA

E-mail: Wenchuan Liang - wliang@cmgm.stanford.edu; Lucila S Licate - lsl4@po.cwru.edu; Hans M Warrick - warrick@cmgm.stanford.edu; James A Spudich - jspudich@cmgm.stanford.edu; Thomas T Egelhoff* - tte@po.cwru.edu

*Corresponding author

Abstract

Background: Cortical myosin-II filaments in *Dictyostelium discoideum* display enrichment in the posterior of the cell during cell migration and in the cleavage furrow during cytokinesis. Filament assembly in turn is regulated by phosphorylation in the tail region of the myosin heavy chain (MHC). Early studies have revealed one enzyme, MHCK-A, which participates in filament assembly control, and two other structurally related enzymes, MHCK-B and -C. In this report we evaluate the biochemical properties of MHCK-C, and using fluorescence microscopy in living cells we examine the localization of GFP-labeled MHCK-A, -B, and -C in relation to GFP-myosin-II localization.

Results: Biochemical analysis indicates that MHCK-C can phosphorylate MHC with concomitant disassembly of myosin II filaments. In living cells, GFP-MHCK-A displayed frequent enrichment in the anterior of polarized migrating cells, and in the polar region but not the furrow during cytokinesis. GFP-MHCK-B generally displayed a homogeneous distribution. In migrating cells GFP-MHCK-C displayed posterior enrichment similar to that of myosin II, but did not localize with myosin II to the furrow during the early stage of cytokinesis. At the late stage of cytokinesis, GFP-MHCK-C became strongly enriched in the cleavage furrow, remaining there through completion of division.

Conclusion: MHCK-A, -B, and -C display distinct cellular localization patterns suggesting different cellular functions and regulation for each MHCK isoform. The strong localization of MHCK-C to the cleavage furrow in the late stages of cell division may reflect a mechanism by which the cell regulates the progressive removal of myosin II as furrowing progresses.

Background

Most animal cells are constantly rearranging their cellular structures to optimally perform their functions or to respond appropriately to the changing environment that surrounds them. Using a simple protein "building block" that has the ability to self-associate to form massive structural arrays is a common theme used in creating a dynamic cytoskeleton. Temporal and spatial regulation of this self-assembly and its associated disassembly process is critical for correct function. For a model system, we have

focused on the dynamics of myosin II thick filaments in *D. discoideum*. This protein forms a self-assembled, highly regulated bi-directional array of molecules that together with actin filaments are capable of producing force for cellular rearrangements. All evidence suggests that unless this molecule is assembled into its appropriate thick filament array it cannot function to produce force.

Eukaryotic cells during cell division construct contractile rings that are mainly composed of an actin-based cytoskeleton. Myosin II, a key component of this actin-based cytoskeleton, has been shown to be essential for cytokinesis of *D. discoideum* cells in suspension as well as for efficient chemotaxis and morphogenetic changes in shape during development) [1–3]. All of these roles require myosin II to be in the form of thick filaments. The question of how myosin II thick filament assembly is regulated within living cells, however, remains mostly unanswered. The amoeba *D. discoideum* has a number of advantages as a model system to study in vivo regulation of myosin II thick filament assembly. *D. discoideum* has only one endogenous copy of the myosin II heavy chain gene, and null strains of myosin II are available) [1,2]). Cytokinesis in *D. discoideum* is also morphologically very similar to that of animal cells)[4].

In *D. discoideum*, myosin II molecules are constantly relocating into multiple locations for participating in various processes. Dynamic exchange occurs between a cytosolic soluble pool and assembled filaments that are enriched in the cortical cytoskeleton. The half-life of myosin between these pools has been measured to be ∼ 7 sec, indicating the importance of dynamic assembly control in the localization of the protein)[5]. When a cell migrates, myosin II accumulates in the posterior of the cell. During cell division, myosin II accumulates in the cleavage furrow in the early stages of cytokinesis. To accomplish its cellular tasks, myosin II assembles into bipolar thick filaments and pull together oppositely oriented actin filaments to produce contractile forces. Mutant forms of myosin II that do not assemble into bipolar thick filaments in vitro fail to rescue myosin null phenotypes, nor do they localize to the furrow during cytokinesis [6,7]. Although myosin II is not essential for cell division on a surface, it is critical for normal timely cell separation and for symmetric placement of the division furrow [8]. GFP-myosin II is transported to the furrow of dividing cells growing on surfaces even though it is not essential for cytokinesis under these conditions.

The assembly of myosin II monomers into filaments is regulated by phosphorylation of its heavy chains at three threonine residues at the C-terminus of the tail [9,10]. Dephosphorylation of these threonines is a prerequisite of filament assembly, as confirmed by the phenotypes of a

3xAsp mutant, in which the three threonines are replaced by three aspartate residues (mimicking the phosphorylated state) [11]. In vitro the 3xAsp myosin II is severely impaired for filament assembly, and in vivo 3xAsp myosin II fails to assemble or localize to the cortical cytoskeleton. Cells expressing this myosin thus recapitulate the defects of myosin II null cells, including failure to develop normally and failure to divide in suspension. In contrast, cells expressing a non-phosphorylatable myosin II construct (3xAla myosin cells) display severe myosin overassembly into the cytoskeleton [11], and excessive myosin localization to the cleavage furrow during cytokinesis [7]. The 3xAla myosin cells also display severe defects in chemotactic cell migration, demonstrating the importance of proper myosin II assembly dynamics in this process [12].

Myosin II heavy chain kinase (MHCK) activity in this system capable of disassembling myosin II filaments in vitro was originally reported with partially enriched kinase fractions [13]. The enzyme MHCK-A was subsequently purified to homogeneity and shown to be capable of driving myosin II filament disassembly in vitro via myosin II heavy chain phosphorylation [14,15]). A MHCK-A cDNA was cloned via expression cloning and peptide sequence derived from the native enzyme [16]. This enzyme is now recognized as the founding member of a highly novel family of protein kinases unrelated to conventional protein kinases, with members present in *D. discoideum* and throughout the animal kingdom. Homology-based cloning and genomic approaches led to the identification of two closely related *D. discoideum* enzymes, MHCK-B [17] and MHCK-C (GenBank accession AAC31918, and [18]). Several enzymes present in mammalian systems are now recognized as having the same conserved catalytic domain, including the eEF-2 kinases [19][20] and TRP-PLIK, a bifunctional protein with kinase and ion channel activities [21]. Biochemical analysis with MHCK-B has confirmed that this enzyme phosphorylates *D. discoideum* myosin II in vitro [17,22]). Analysis reported here confirms that MHCK-C also readily phosphorylates *D. discoideum* myosin II in vitro, supporting a possible direct role for this enzyme in myosin II localization control in vivo.

Although substantial biochemical analysis has been performed with this family of *D. discoideum* MHCKs, there is relatively little information on the cellular distribution of the endogenous MHCKs in vivo. Previously, Steimle and colleagues [23] reported that in interphase cells, during chemotaxis, random migration, and endocytic/phagocytic events, MHCK-A is recruited preferentially to anterior F-actin rich protrusions. With the discovery of two additional myosin II heavy chain kinases, MHCK-B and MHCK-C, we report here in live migrating and cytokinetic cells a systematic in vivo examination of these three MHCKs labeled with GFP.
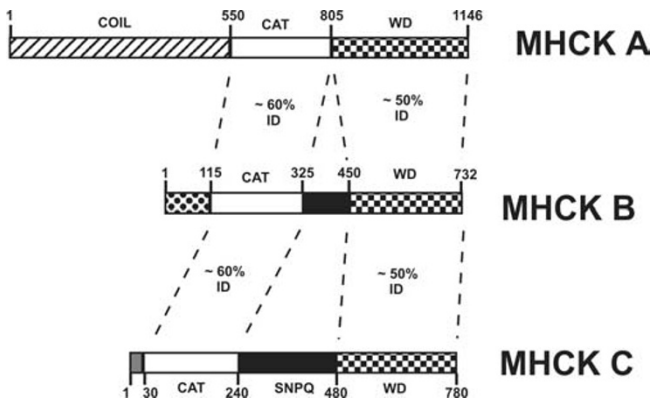
Figure 1
Domain organization of Dictyostelium MHCKs. All three enzymes contain a strongly conserved seven-fold WD repeat domain at the carboxyl-terminus. MHCK-A has a unique amino-terminal domain of ~ 500 residues that forms a coiled-coil domain responsible for oligomerization and for localization to anterior actin-rich cell extensions. MHCK-B has an amino-terminal segment of ~ 115 residues of currently unknown function. GFP was fused at the amino-terminus of each MHCK for the studies presented here (at codon 2 in each case). "CAT" indicates position of the conserved protein kinase catalytic domain in each enzyme. "SNPQ" (black boxes) indicates position of segments of MHCK-B and MHCK-C that display low amino acid complexity and are rich in serine, asparagine, proline, and glutamine residues.

This analysis reveals striking differences in localization between these three enzymes. During cytokinesis, MHCK-A displays weak enrichment at the cell poles, while MHCK-B displays a mostly diffuse localization. In contrast, MHCK-C displays strong localization to the cleavage furrow only during the late stages of cell division. These results suggest that *D. discoideum* cells use a family of related MHCKs to modulate myosin II filament assembly, each with distinct roles.

Results

MHCK domain organization and MHCK C biochemical activity

The enzymes MHCK-A and MHCK-B have established roles in the control of *D. discoideum* myosin filament assembly both in vitro and in vivo [16,17,24], and Egelhoff, T. T., (unpublished studies). These enzymes have a conserved domain organization that includes a highly novel protein kinase catalytic domain unrelated to conventional kinases, and a carboxyl-terminal WD repeat domain that targets these enzymes to myosin II filaments (Figure 1). Genomic sequence corresponding to the related enzyme MHCK-C was deposited in GenBank by Loomis and colleagues (accession number AAC31918). MHCK-C differs from MHCK-A and MHCK-B in that it lacks any significant amino-terminal domain upstream of the catalytic do-

main; conserved catalytic domain residues are present within approximately 30 residues of the methionine start codon of MHCK-C (Figure 1). Of this set of enzymes, MHCK-C is also unique in that it contains a large central domain of approximately 30 kDa that consists of highly repetitive stretches rich in serine, asparagine, proline, and glutamine. However, the strong similarity of MHCK-C to MHCK-A and MHCK-B in the conserved catalytic domain and the carboxyl-terminal WD repeat domain suggested that it might represent a third myosin heavy chain kinase in this organism.

To test this possibility at the biochemical level, we engineered and expressed an epitope-tagged construct that contains an amino-terminal FLAG epitope fused to codon 2 of MHCK-C. FLAG-MHCK-C was purified using a combination of ammonium sulfate fractionation and FLAG-peptide affinity chromatography. Purified FLAG-MHCK-C was subjected to SDS-PAGE. Western blot analysis with anti-MHCK-C polyclonal antibodies (Figure 2A) and with anti-FLAG monoclonal antibodies (not shown), and Coomassie staining (Figure 2A) confirmed the purification of the expressed protein, migrating at the correct size for MHCK-C. The FLAG-MHCK-C protein consistently suffered proteolytic cleavage during purification. In initial lysates, the major immunoreactive species migrated at ~ 100 kDa, but during purification a major clipped species formed with a size of ~ 35 kDa (Figure 2A). This species reacted with both anti-MHCK-C antisera and with anti-FLAG epitope antibodies (not shown), indicating this fragment to be an amino-terminal domain of MHCK-C. Addition of protease inhibitors during purification reduced but did not eliminate formation of this clipped MHCK-C.

Purified FLAG-MHCK-C readily phosphorylated native *D. discoideum* myosin II on the myosin heavy chain (MHC) in vitro (Figure 2B and 2C). No incorporation was detected on autoradiographs at the mobility of myosin light chains, supporting the model that MHCK-C, like MHCK-A, modulates filament assembly and not myosin motor activity (data not shown). To determine whether phosphorylation by MHCK-C affected myosin II assembly properties, samples of purified *D. discoideum* myosin II were incubated with MHCK-C in the presence and absence of ATP. Samples were then subjected to centrifugation to sediment myosin II filaments, and the proportion of myosin II in the pellet in each sample was quantified using SDS-PAGE and Coomassie blue staining as a measure of filament assembly (Figure 3A). Incubation of myosin II with MHCK-C in the absence of ATP resulted in assembly levels typical for purified *Dictyostelium* myosin, with 82% of the myosin sedimenting in the current set of assays (Figure 3B). Incubation of myosin II with MHCK-C in the presence of ATP resulted in substantial filament dis-
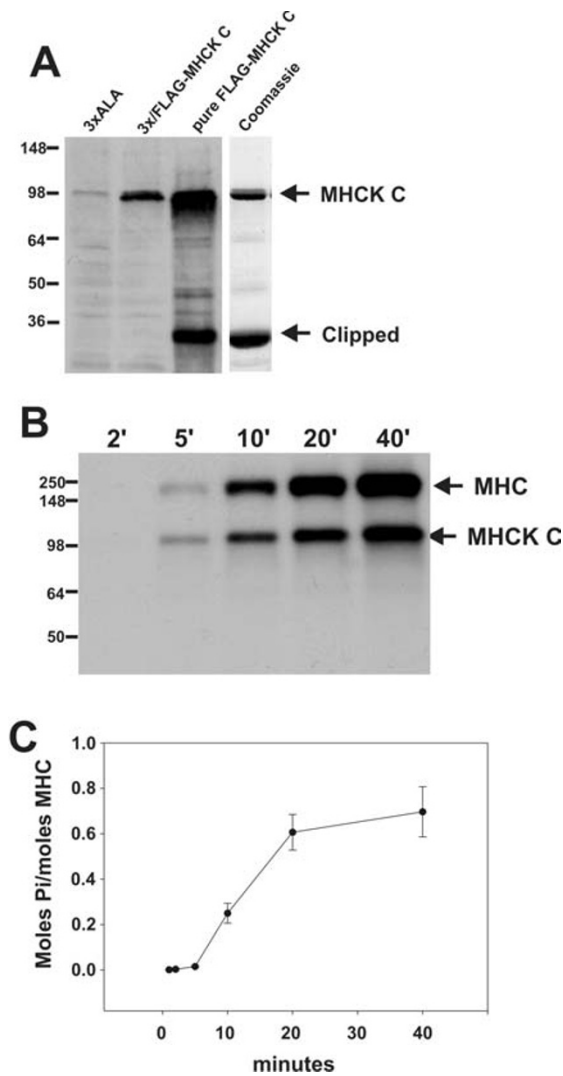
Figure 2
Purification and activity of epitope-tagged MHCK-C.
A. MHCK-C expression levels are indicated by western blot analysis of total cell lysates of the 3xALA parental cell line (3XALA lane) and lysates of 3xALA cell overexpressing FLAG-MHCK-C (3x/FLAG-MHCK-C lane). Immunoreactivity of purified FLAG-MHCK-C indicates presence of full length and clipped FLAG-MHCK-C (pure FLAG-MHCK-C lane). Coomassie blue stained material (Coomassie lane) indicates purity and the presence of a clipped breakdown catalytic domain fragment migrating at ~ 35 kDa. Western blot performed with polyclonal antisera generated against the catalytic domain of MHCK-C. B. FLAG-MHCK-C both autophosphorylates and phosphorylates *Dictyostelium* myosin II on the heavy chain. C. Kinetics and stoichiometry of myosin heavy chain (MHC) phosphorylation by FLAG-MHCK-C. For panels B and C phosphorylation was performed in a reaction mixture consisting of 500 nM MHC (in the form of native myosin II), 100 nM FLAG-MHCK-C, 0.5 mM ATP, 2 mM $MgCl_2$, and 20 mM TES pH 7.0. Error bars represent S.E.M., n = 3
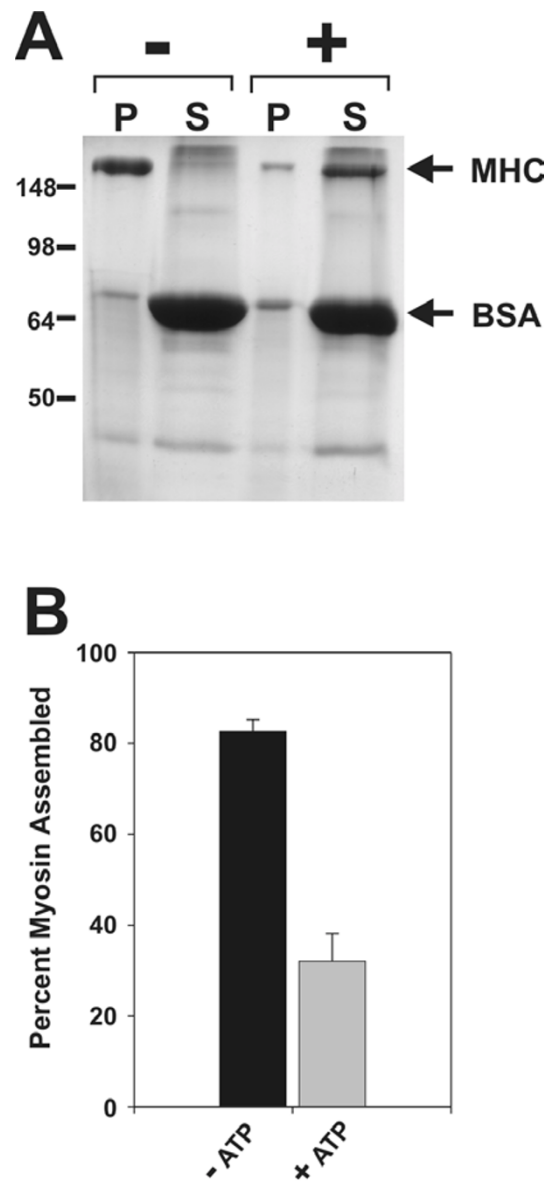

Figure 3
Phosphorylation of myosin II by FLAG-MHCK-C drives filament disassembly. Myosin II was subjected to phosphorylation by FLAG-MHCK-C as for experiments in figure 2. A. Samples containing myosin II (500 nM MHC concentration), FLAG-MHCK-C (100 nM), and BSA (1 μg/μl) were incubated either without ATP (-) or with ATP (+) for 30 minutes, adjusted to 50 mM NaCl for optimal myosin II filament assembly, then subjected to sedimentation at 90,000 ×g for 10 min to pellet assembled filaments. Equal fractions of pellets (P) and supernatants (S) were subjected to SDS-PAGE and Coomassie blue stain. Disassembly is reflected as a loss of MHC in the pellet fractions. No disassembly of myosin occurs if ATP is added in the absence of FLAG-MHCK-C (not shown). B. Densitometric quantification of the percent myosin II in the pellet fractions. Error bars represent S.E.M., n = 5.

assembly, with only 32% of the myosin II sedimenting following phosphorylation. These results confirm that MHCK-C can phosphorylate myosin II, and that this phosphorylation is capable of driving filament disassembly in vitro.

Myosin II phosphorylation experiments revealed two additional features of MHCK-C biochemical behavior. First, FLAG-MHCK-C autophosphorylates during the course of in vitro phosphorylation reactions (Figure 2B). Second, the activity of FLAG-MHCK-C appears to be very low in the initial stages of in vitro phosphorylation reactions, but then rises after approximately 5 minutes (Figure 2C). These attributes are reminiscent of the behavior of MHCK-A, which upon purification exists in an unphosphorylated low activity state. In vitro autophosphorylation of MHCK-A was found to increase the V_{max} of the enzyme 50-fold [25]. To test for similar autophosphorylation regulation of MHCK-C, we tested the activity of FLAG-MHCK-C with and without an initial autophosphorylation step, towards the peptide substrate MH-1 (a 16-residue peptide corresponding to one of the mapped MHC phosphorylation target sites for MHCK A in the myosin tail). If FLAG-MHCK-C was not subjected to a pre-autophosphorylation step, ^{32}P incorporation into the peptide displayed a similar lag phase as observed for myosin II phosphorylation (Figure 4A and 4B, open symbols). If FLAG-MHCK-C was pretreated with Mg-ATP for 10 min at room temperature, the lag phase for peptide phosphorylation was eliminated (figure 4A and 4B, closed symbols). These results support the model that autophosphorylation activates MHCK-C. Another feature reported earlier for MHCK-A activation is that myosin II itself stimulates autophosphorylation [25]. To test whether MHCK-C autophosphorylation is accelerated in the presence of myosin II, the stoichiometry of FLAG-MHCK-C autophosphorylation was evaluated in the presence and absence of myosin II filaments. Under the assay conditions here, myosin II did not significantly stimulate the rate of FLAG-MHCK-C autophosphorylation (Figure 4C). This result suggests that MHCK-C may be regulated in vivo by mechanisms distinct from those that regulate the activity of MHCK-A.

MHCKs have different subcellular localizations in interphase cells
To gain insights into the relative cellular roles and localization of MHCK-A, MHCK-B, and MHCK-C, we have evaluated the behavior of GFP fusions corresponding to each of these enzymes. Distribution of GFP-labelled MHCKs (GFP-MHCK-A, -B and -C) was examined in live AX2 cells (containing an endogenous mhcA gene). These GFP-MHCK expressing cells were able to sporulate and grow in suspension, indicating that at the expression level of these clonal cell lines, the expression of GFP-MHCKs in the AX2 cells does not detectably change myosin II expression or
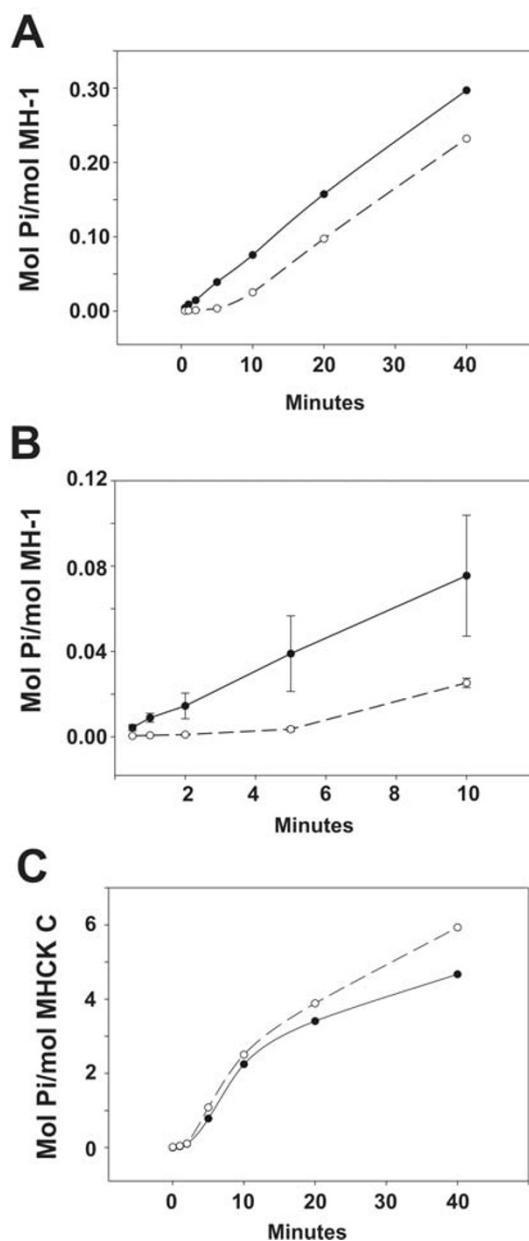

Figure 4
FLAG-MHCK-C is activated by autophosphorylation. The peptide substrate MH-1 is a 16 residue peptide that corresponds to the mapped myosin II phosphorylation site at position 2029 of MHC. A. Phosphorylation of MH-1 by FLAG-MHCK-C occurs with a reproducible lag phase (open symbols), similar to the lag seen with myosin II as the substrate. Preincubation of FLAG-MHCK-C with MgATP eliminates the lag phase (closed symbols). Phosphorylation is plotted in terms of moles Pi transferred as fraction of total moles MH-1 peptide in reaction. B. Expanded plot of early time points of the same experiment. Bars represent S.E.M., n = 3. C. Addition of myosin II to FLAG-MHCK-C autophosphorylation reactions does not accelerate MHCK-C autophosphorylation.
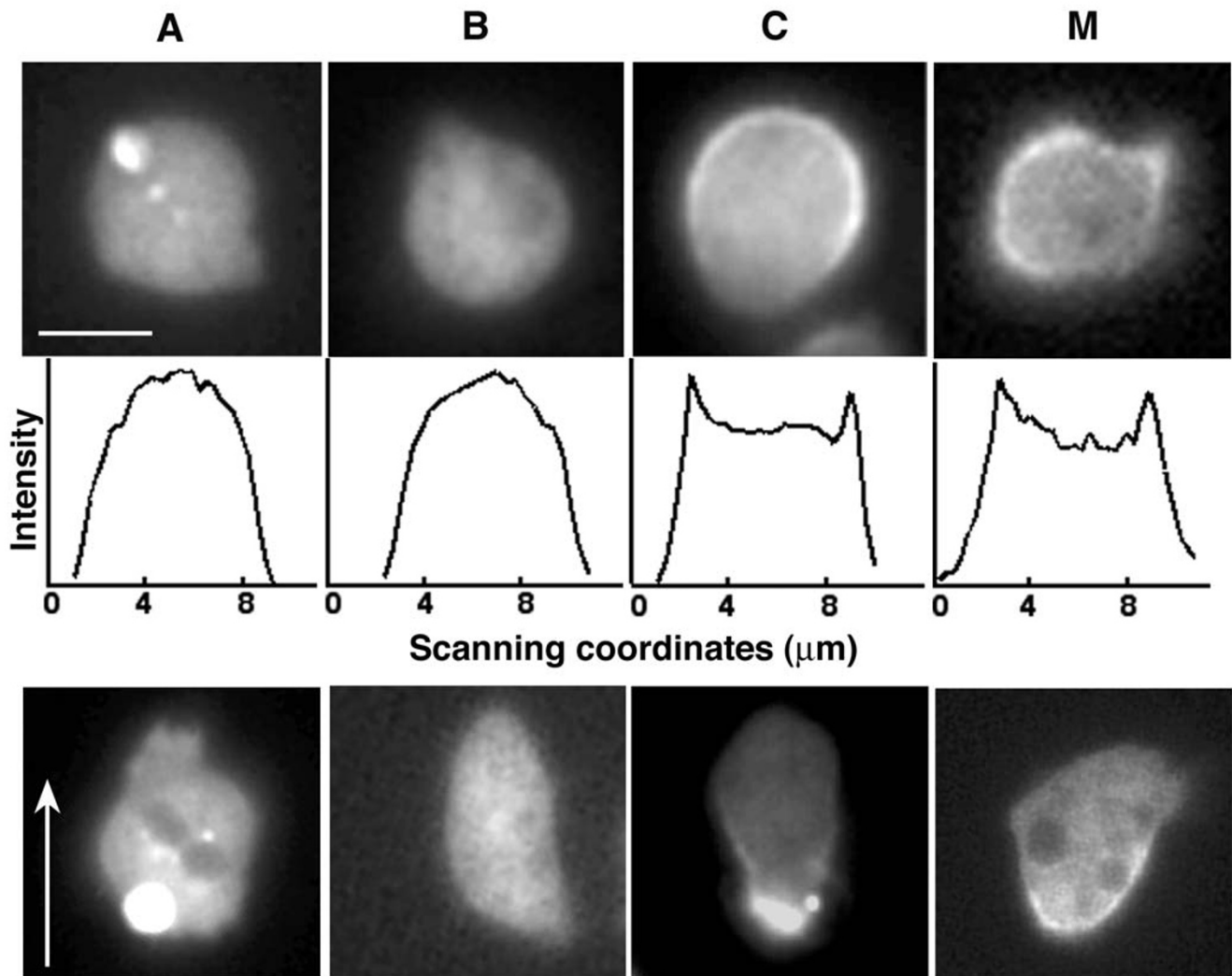
Figure 5
Comparison of interphase *D. discoideum* cells. GFP-MHCK-A (A), GFP-MHCK-B (B), and GFP-MHCK-C (C) are expressed in Ax2 cells. GFP-myosin II (M) is expressed in myosin II null cells. Scale bar equals to 5 μm. Quantification of the increased accumulation of GFP-proteins in the cortex is obtained by line-scans of the fluorescent intensity profiles across the center of cells (middle row). The x-axis is the scanning coordinate in a unit of μm, and the y-axis is the fluorescence intensities in an arbitrary unit. Interphase cells moving in the upward direction show that GFP-MHCK-A localizes transiently to the anterior pseudopod (A, bottom), while GFP-MHCK-C and GFP-myosin II stay in the posterior region of the cells (C and M, bottom, respectively). GFP-MHCK-B, on the other hand, is homogeneously cytosolic (B, bottom). The brighter cells expressing any of these GFP constructs sometimes display intense fluorescent spots (as in A, top and bottom, and B, bottom) that are likely non-physiological aggregates of the overexpressed protein, as discussed previously [23]. A time-lapse movie in Quicktime format illustrating the anterior localization behavior of MHCK A is available as an additional file (see additional file 1).

function. The fluorescence distributions of these cells were compared with cells expressing GFP-myosin II, obtained by transforming myosin null cells with a plasmid that carries GFP-mhcA-containing plasmid p102 (Materials and Methods) designated as GFP-myosin II cells hereafter.

The localization pattern of the GFP-MHCKs in the presence of myosin II was first compared to the distribution of GFP-myosin II cells in interphase (Fig. 5). Many cells of each transformation were examined (n > 50) and examples of the distribution of GFP-MHCK-A (Fig. 5-A, top), GFP-MHCK-B (Fig. 5-B, top) and GFP-MHCK-C (Fig. 5-C, top) are shown. GFP-myosin II distributed in the cyto-
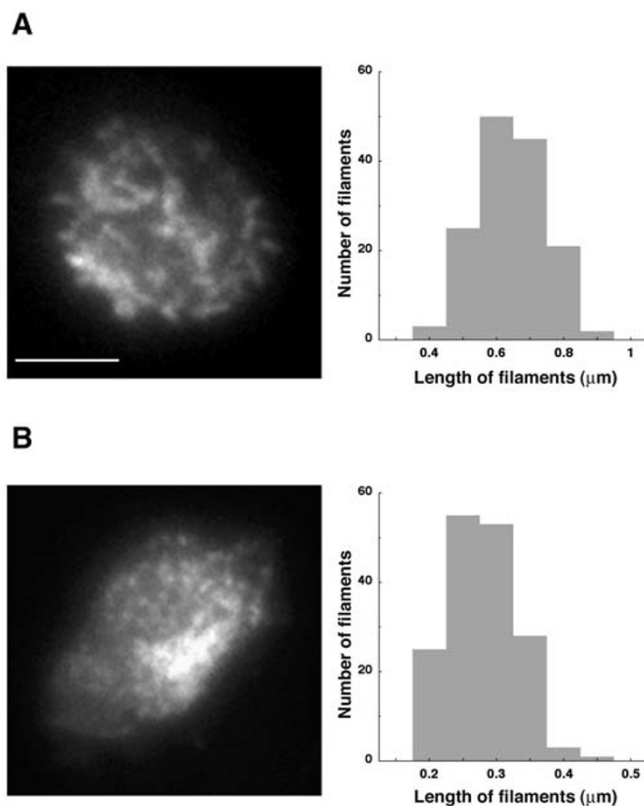
Figure 6
TIRF images of GFP-myosin II (A) and GFP-MHCK-C expressed in the presence of myosin II (B). The fluorescent images show GFP-myosin II thick filaments and GFP-MHCK-C particles in the cortex of a cell attached on a coverslip with a refractive index of 1.78. The distribution of the rod length is displayed next to the images. The mean length of GFP-myosin II and GFP-MHCK-C is 0.6 and 0.3 μm, respectively. The scale bar is 3 μm.

plasm and enriched in a cortical layer in interphase as has been described earlier [7] is shown in Fig. 5-M (top). GFP-labelled MHCK-A and B distributed in the cytoplasm, and appeared to be excluded from the area that corresponded to nucleus. In contrast to GFP-Myosin II, GFP-labelled MHCK-A and B did not concentrate in the cell cortex (Fig. 5-M, top). Pixel intensities on a line drawn through the center of the cells allow a more quantitative comparison of the enrichment of GFP-MHCKs. A cortical distribution shows a distinctively increased accumulation of GFP fluorescent intensity at the cell edges, displaying two peaks flanking the cell cross-section as seen in the case of the GFP-myosin II cells (Fig. 5-M, middle). Out of the three MHCKs, only GFP-MHCK-C appeared to be concentrated in the cell cortex (Fig. 5-C, top), and had the fluorescent profiles containing the two flanking peaks (Figure 5-C, middle). GFP-MHCK-C also appears to be excluded from

the nucleus, similar to that seen in cells expressing GFP-myosin II.

In free-moving cells, GFP-MHCK-A was frequently transiently enriched in the protruding edge (Fig. 5-A, bottom), and hence results in rather noticeable pseudopods at the anterior region compared with that in the GFP-myosin II cells. A time-lapse movie in Quicktime format illustrating this behavior is available as an additional file (see additional file 1). GFP-MHCK-B, however, displayed no indication of transient enrichment in any part of the cells while moving; instead it distributes homogeneously within cells (Fig. 5-B, bottom). The cells expressing GFP-MHCK-B appeared to have smooth cell edges because the fluorescence did not label the dynamic pseudopods at the leading edge of the cell, compared with that in GFP-MHCK-A cells. In contrast to MHCK-A and MHCK-B distribution, GFP-MHCK-C was frequently enriched in the posterior cortex of the moving cells (Fig. 5-C, bottom), as seen also for GFP-myosin II (Fig. 5-D, bottom). GFP-MHCK-C occasionally displayed transient enrichment in pseudopodial extensions as well (data not shown).

Dynamic localization of GFP-myosin II and GFP-MHCK-C in the cortex of living D. discoideum cells
As shown above, in interphase GFP-myosin II and GFP-MHCK-C expressed in the presence of myosin II both concentrate in the cell cortex. The actin-rich cortex is estimated to be approximately 0.1–0.2 μm thick in *D. discoideum* cells [26], similar to the thickness in other eukaryotic cells [27]. This dimension makes total internal reflection fluorescence (TIRF) microscopy an attractive tool to examine cortical GFP-labelled proteins at the cell-surface contacts. Total internal reflection occurs when light travelling in a medium with high refractive index encounters a medium with low refractive index beyond the critical angle, determined by the ratio of the two refractive indices according to the Snell's law [28]. In our experiments, the coverslip and the cells represent the media with high and low refractive indices, respectively. Under this condition, there is still an exponentially-decayed, evanescent wave penetrating into the *D. discoideum* cells. The typical depth of the evanescent wave is in the range of 100–200 nm away from the coverslip, which is suitable for exciting cortical GFP-proteins in living *D. discoideum* cells.

As examined by in vitro electron microscopy, negatively stained purified wild-type myosin II molecules formed bipolar thick filaments 0.6–0.8 μm in length [29]. Filament structures of similar size have also been observed via immunofluorescent microscopic observation of fixed cells [30]. Examination of live, GFP-myosin II expressing cells with a TIRF microscope (Fig. 6A) shows an accumulation of fluorescent rod-like shapes with an estimated length to be approximately 0.64 μm (standard deviation = 0.10, n =

146). This dimension is consistent with myosin II thick filaments measured from the in vitro electron microscopy photographs [29]. Using TIRF microscopy, these structures, putative filaments, are not apparent in GFP-3xAsp myosin II cells in which the three potential Thr phosphorylation targets have been replaced with Asp residues (data not shown). As this MHC mutation inhibits filament assembly [11], the inability of GFP-3xASP myosin to form such structures suggests that these TIRF-resolved structures are discrete myosin II filaments. Our TIRF analysis furthermore indicated that a few of the GFP-myosin II thick filaments move dynamically. Some filaments moved a long distance across the field with a velocity up to approximately 0.4 μm/sec before stopping. Other filaments seemed to be confined to a small region and eventually disappeared.

GFP-MHCK-C expressing cells (in the presence of myosin II), display punctate aggregates of fluorescence, with the longer dimension approximately 0.30 μm (standard deviation = 0.05, n = 165, Fig. 6B). The shorter dimension is about 0.15–0.2 μm, similar to what was observed in myosin II thick filaments. The GFP-MHCK-C fluorescent aggregates showed dynamic motility similar to that of GFP-myosin II aggregates. These structures could not be detected when GFP-MHCK-C was expressed in myosin II null cells (data not shown), suggesting that the formation of the GFP-MHCK-C punctate aggregates is myosin II-dependent.

Differential localization of GFP-MHCKs during cytokinesis

At the early stage of cytokinesis, GFP-myosin II reorganizes and is concentrated into the region that flanks the furrow located at the equatorial region of the dividing cells (Fig. 7-M, top). As the two daughter cells continue to separate (denoted the late stage of cytokinesis), GFP-myosin II persists in this zone, which becomes the posterior region of each of the two forming daughter cells (Fig. 7-M, bottom). GFP-myosin II, on the other hand, was not enriched in the polar region and therefore the polar regions displayed a smooth contour in fluorescent images, as described earlier [7].

Neither GFP-MHCK-A (Fig. 7-A) or -B (Fig. 7-B) was observed to be concentrated in the furrow region during any stage of cytokinesis; nor did they localize to the posterior region of the two daughter cells at the late stage of cytokinesis. Instead, GFP-MHCK-A was enriched in the protrusions extending from the poles of the dividing cells, which resulted in a more prominent appearance of the ruffling polar pseudopods throughout the cytokinesis process. GFP-MHCK-B, however, stayed homogeneously cytoplasmic during cytokinesis without any sign of enrichment in any region. It was excluded from the polar protrusions, as seen by the smooth contour of the poles (Fig. 7-B). Inter-

estingly, as the cells progressed from the early to late stages of cytokinesis, GFP-MHCK-B appeared to be excluded from the furrow (Fig 7-B), as compared to the appearance of GFP-MHCK-A or GFP-MHCK-C.

The localization pattern of GFP-MHCK-C was different from the other two kinases (Fig. 7-C). At the early stage of cytokinesis, GFP-MHCK-C generally displayed a cytosolic distribution with some uniform cortical enrichment, but showed no sign of furrow concentration. However, at the late stage of cytokinesis, as soon as the two daughter cells begin to separate from each other, GFP-MHCK-C became detectable at the newly formed posterior regions of the two daughter cells. The spatial localization of GFP-MHCK-C is similar to that observed for GFP-myosin II at the late stage of cytokinesis (Fig. 7-B and 7-M). In summary, these three GFP-MHCKs have distributions that are temporally and spatially different, as summarized in the sketches shown in Figure 7 bottom.

To further illustrate the differential temporal localization, images of two cells expressing GFP-MHCK-C are compared to a cell expressing GFP-myosin II from the interphase (I, Figure 8) to the fully divided daughter cells (D, Figure 8). During interphase, all three cells display cortical distribution of the GFP-labeled proteins. When the cells progress into the quiescence stage (Q; equivalent to mid-mitosis), GFP-MHCK-C loses its cortical enrichment while GFP-myosin II typically remains cortical. When the cells begin to elongate (E, Figure 8), GFP-myosin II already concentrates at the equatorial region and remains there through the early stage (C_e, Figure 8), the mid-stage (C_m, Figure 8), and the late stage of cytokinesis. GFP-MHCK-C, however, displays no sign of furrow localization until the late stage of cytokinesis, when it suddenly appears at the posterior region of the daughter cells and stays for the duration of cell division (D). Time lapse movies in Quicktime format corresponding to each series in figure 8 are available as additional files (see additional file 2, additional file 3, and additional file 4).

Localization of GFP-MHCKs in the absence of myosin II

To understand whether the differential distribution observed on GFP-MHCK-A, -B and -C cells depended on the existence of myosin II, we expressed these kinases in myosin II null cells and compared the localization patterns. GFP-MHCK-A and -B showed identical localization in both interphase and cytokinesis cells regardless of the presence of myosin II in the cells (data not shown). GFP-MHCK-C, however, failed to localize to the cortex in interphase cells (Fig. 9-C, M null, top), and the two characteristic peaks were missing in the linescan. During free movement in the absence of myosin II, GFP-MHCK-C was not enriched in the posterior region of the cells (Fig. 9-C, M null, bottom). At the early stage of cytokinesis in my-
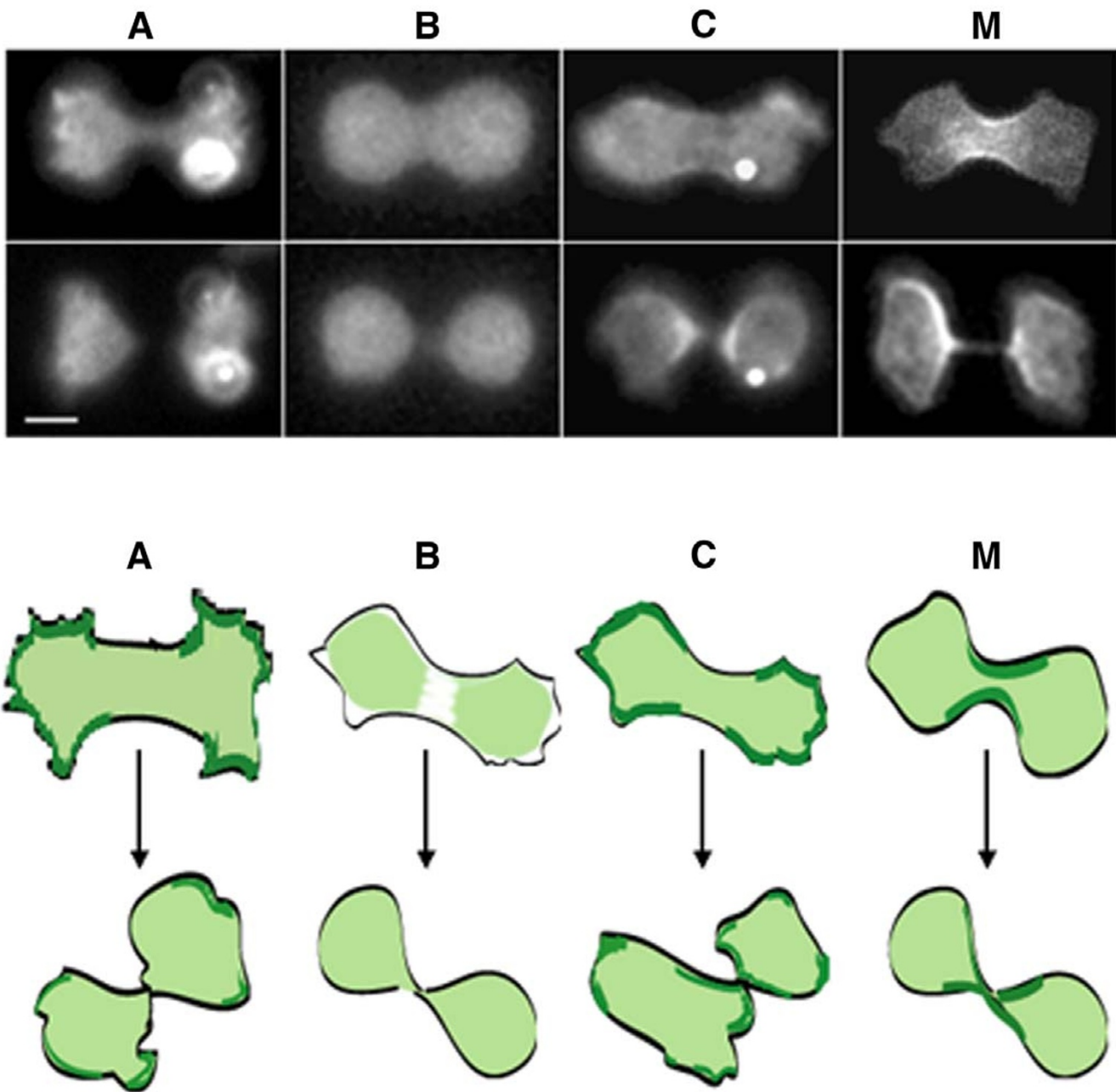
Figure 7
Comparison of GFP-MHCKs and GFP-myosin II distribution during cytokinesis. In the early-to-mid stage of cytokinesis (upper row), none of the GFP-MHCKs localizes to the furrow, opposite to that of the GFP-myosin II (M). GFP-MHCK-A and -C, instead, enriches to the polar protrusions at this stage (A and C, upper row). At the later stage of cytokinesis (lower row), GFP-MHCK-C suddenly appears at the posterior region of the two daughter cells (C), similar to what is observed for GFP-myosin II cells (M). The scale bar shown in the image is 5 μm. The observation described is summarized in the sketch shown below the images.
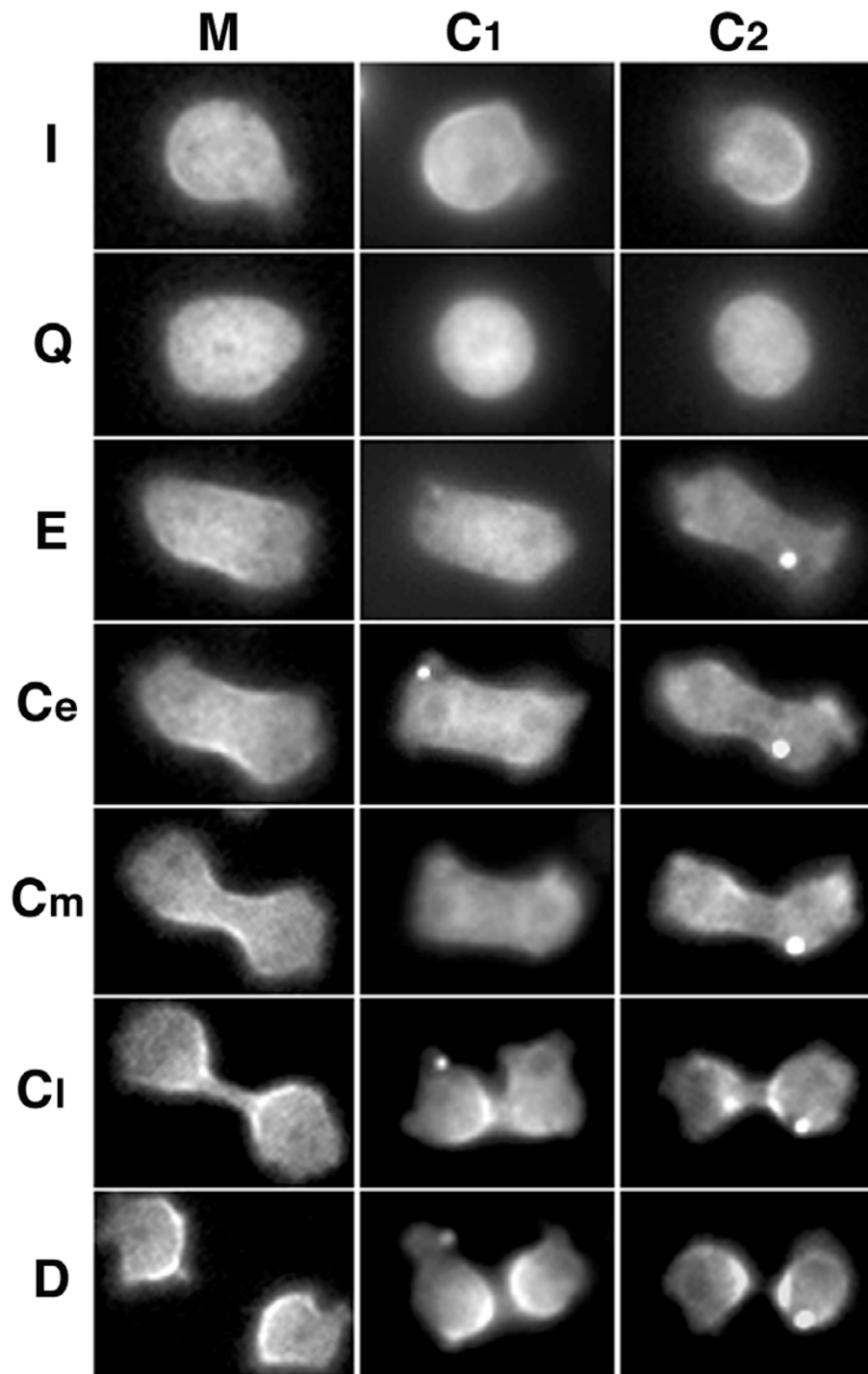
Figure 8
MHCK-C and Myosin II localization at each stage of cytokinesis. Image comparison of cells expressing GFP-MHCK-C (C_1 and C_2) with GFP-myosin II (M) from the interphase (I), the quiescence (Q), the elongation (E), through the early stage (C_e), the mid-stage (C_m) and the late stage (C_l) of cytokinesis, and finally to the fully divided (D) daughter cells. Although GFP-myosin II localized to the equatorial region early on at the elongation stage and through the whole stages of cytokinesis, GFP-MHCK-C does not appear until the late stage of cytokinesis (C_l). Time lapse movies in Quicktime format corresponding to each series in figure 8 are available as additional files (see additional file 2, additional file 3, and additional file 4).
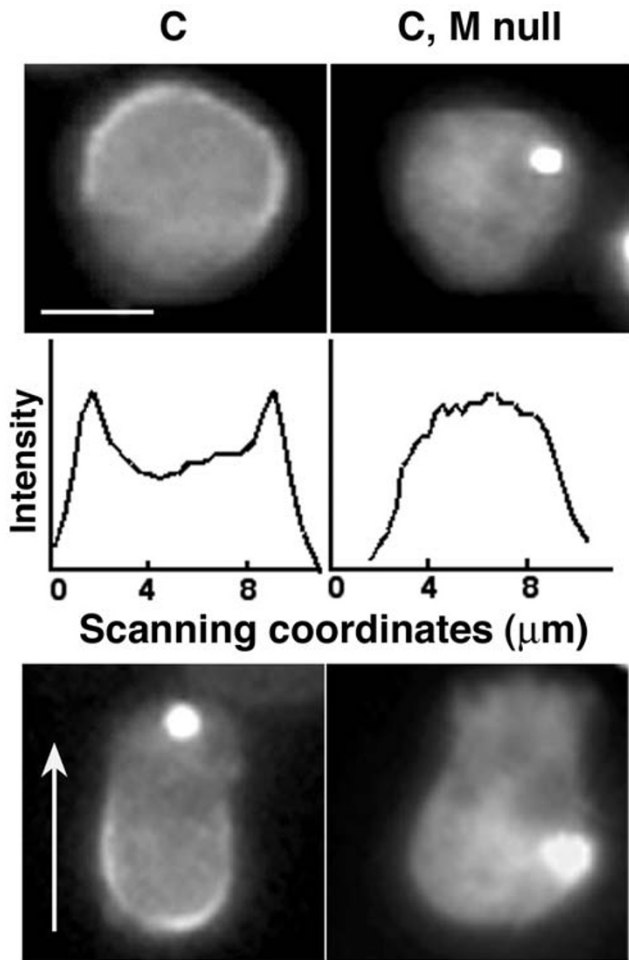
Figure 9
Comparison of GFP-MHCK-C distribution patterns in the interphase of Ax2 (C) and myosin II null (C, M null) cells. In the absence of myosin II, GFP-MHCK-C does not localize to the cell cortex (C, M null, top). A line-scan of the fluorescent intensity profiles across the cells also indicates no cortical distribution in the absence of myosin II (C, M null, middle), the units of x- and y-axis are the same as in Figure 1. In moving cells, direction indicated by arrow, GFP-MHCK-C expressed in the presence of myosin II enriches at the posterior region (C, bottom), GFP-MHCK-C expressed in the myosin II null cells does not stay at the posterior of the cells (C, M null, bottom). The scale bar is 5 μm.

osin II null cells, GFP-MHCK-C was not enriched the furrow region (figure 10, top), similar to what was observed in the presence of myosin II as shown in Figure 7-C, top. However, when myosin II null cells progressed to the late stage of cell separation, GFP-MHCK-C was never localized to the constricting furrow or to the forming posterior region of the two daughter cells (Fig. 10-C, M null, bottom).

Discussion

The results reported here provide biochemical and cellular evidence indicating that *D. discoideum* contains a related family of MHC kinase isoforms that display distinct modes of regulation in vitro and distinct localization dynamics in vivo during contractile events, particularly during cytokinesis. Although MHCK-A has been extensively characterized at the biochemical level [18,22,25,31], only limited biochemical analysis has been performed with bacterially-expressed subdomains of MHCK-B and MHCK-C [17,18,22]. The current biochemical results provide strong support for the hypothesis that MHCK-C acts as a MHC kinase in vivo. Further studies with second messenger compounds may help to identify upstream physiological mechanisms that regulate MHCK-C autophosphorylation/activation.

Using epi-fluorescence microscopy, we observe strikingly different patterns of dynamic localization for MHCK-A, -B, and -C during polarized migration and cytokinesis. The dynamics of MHCK-C localization are particularly intriguing, with global or posterior cortical enrichment observed during interphase, with a dramatic accumulation in the furrow during late cytokinesis. The apparent absence of MHCK-C from the furrow in early/mid cytokinesis, when myosin II is clearly accumulating, suggests that specific regulatory mechanisms may exist to recruit this enzyme to the furrow during late cytokinesis.

Co-localization of a MHCK with its apparent substrate does not imply that the kinase, in vivo, is actively phosphorylating its substrate. The dynamic localization of a kinase is only one way to regulate its activity. In fact, the MHCKs are very likely to be highly regulated enzymes; previous studies have documented the in vitro regulation of MHCK A by autophosphorylation, myosin filaments, and acidic phospholipids [32], and data presented here documents that MHCK C can also be regulated via autophosphorylation. Further studies are needed to confirm similar regulation in vivo, and to better define the upstream regulatory pathways. With these caveats, the distinct localization patterns for MHCK-A, -B, and -C reported here provide valuable clues as to which spatial and temporal myosin II population may be acted upon by each enzyme.

The dynamics of the three MHCKs also display striking differences in their dependence on myosin II. When the GFP fusions are imaged in myosin II null cells, both MHCK-A and MHCK-B display dynamics indistinguishable from their behaviour in cells wild type for myosin II. In contrast, loss of cortical and furrow localization is seen for GFP-MHCK-C in the absence of myosin II. This result suggests that MHCK-C localization in these settings may be achieved via direct association with myosin II fila-
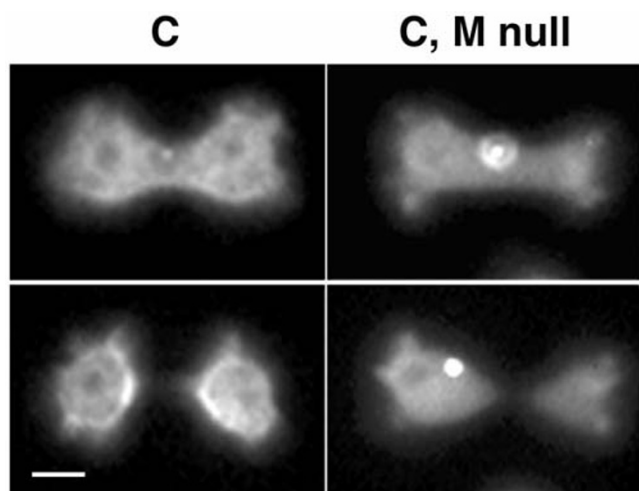
Figure 10
Comparison of GFP-MHCK-C distribution patterns in AX2 (C) and myosin II null (C, M null) cells during cytokinesis. Similar to that expressed in the presence of myosin II, GFP-MHCK-C expressed in the myosin II null cell line does not localize to the furrow at the early stage of cytokinesis (C, M null, upper). However, unlike that expressed in the presence of myosin II, GFP-MHCK-C does not appear at the posterior region of the two leaving daughter cells (C, M null bottom). The scale bar is 5 μm.

ments. Our TIRF studies further support this model, suggesting that MHCK-C may physically associate with myosin II filaments. GFP-MHCK-C under the TIRF microscope displayed short particles with a longer dimension approximately half of the length of myosin II thick filaments. The bare zone of purified wild-type myosin II thick filaments was estimated previously to be in the range of 0.13–0.19 μm [29]. Based upon these results, we suggest that GFP-MHCK-C may colocalize with myosin II thick filaments by binding at the bare zone.

Comparison of the localization pattern between GFP-myosin II and GFP-MHCKs provides us a map of where these three MHCKs localize at different stages in the vegetative cells, as well as how these MHCKs coordinated to ensure proper regulation of myosin II thick filament. Figure 11 depicts our current working model for the dynamics of the three MHCKs during interphase (A), early cytokinesis (B) and late cytokinesis (C). Localization of MHCK-A and MHCK-B does not require myosin II. With or without myosin II, both MHCK-A and MHCK-B are excluded from the cell cortex in interphase; and neither MHCK-A nor MHCK-B colocalize with regions of highest myosin II concentration in moving cells (Fig. 11-A). We suggest that the enrichment of MHCK-A to polar ruffles of dividing cells may represent a mechanism by which *D. discoideum* cells locally disassemble myosin II filaments to facilitate the

polarized recruitment of filaments to the forming contractile ring/furrow zone. This model is consistent with the recent report that MHCK-A displays enrichment into anterior F-actin-rich protrusions of polarized cells during chemotaxis, and into phagocytic and macropinocytotic extensions [23]. The polar localization of MHCK-A would be consistent with the long-standing "polar relaxation" model for cytoskeletal reorganization during cytokinesis [33]. MHCK-A may represent a factor that contributes to polar relaxation in this system via polar disassembly of myosin II filaments. The cytosolic localization of MHCK-B suggests that this enzyme may contribute to a continuous and uniform turnover of myosin II filaments throughout the cell, although it is possible that MHCK-B plays more specific roles in functions yet to be identified.

We suggest that MHCK-C is recruited to the contractile ring during late cytokinesis to facilitate the orderly removal of excess myosin II from the ring as the furrow ingresses. It is particularly intriguing that MHCK-C colocalizes with myosin II in the furrow only at the culmination of cytokinesis where turnover and mobilization of thick filaments might be most appropriate. At this time the cell cycle contraction force requirements are predicted to fall [34] and the cell's geometrical changes would require myosin II thick filaments to disassemble. Although it is clear throughout the animal kingdom and in protozoa that the mass of myosin II in the division furrow decreases steadily with furrow ingression, no mechanism has been identified in any other system that can explain this regulated disassembly. Dynamic changes in MHC phosphorylation levels within the contractile ring have been reported in dividing sea urchin embryos [35], suggesting that MHC phosphorylation as a mechanism regulating furrow myosin II disassembly may occur in other systems besides *D. discoideum*. We suggest that MHCK-C participates in this regulated myosin II filament disassembly in *D. discoideum*, and that this function may be regulated at both the cellular and biochemical level.

Conclusions
We suggest that differential localization of MHCKs occurs in D. discoideum cells for the purpose of regulating myosin II filament assembly levels in the context of specific cellular contractile events such as lamellipodium extension and cytokinetic furrowing. The late appearance of MHCK-C during furrowing suggests a cellular mechanism regulating its localization, and our biochemical data suggest that MHCK-C phosphorylation levels may represent a mechanism for the fine-tuning of the activity of MHCK-C in the cleavage furrow during cell division. This level of regulation could be mediated via second messenger control of autophosphorylation, or via direct MHCK-C phosphorylation by other kinases. Further studies are in progress to test these models.
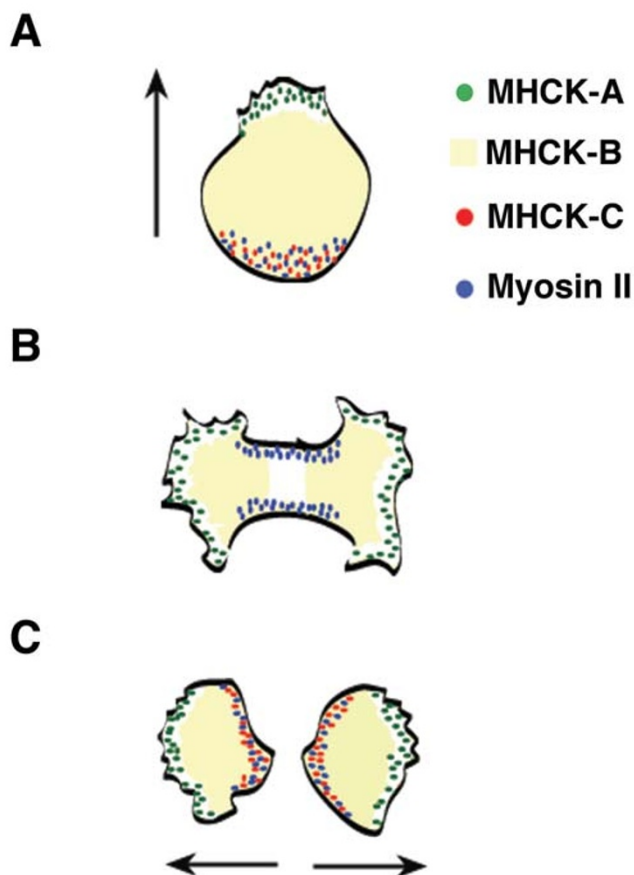
Figure 11
Schematic depiction of differential localization of MHCK-A, -B and -C (in the presence of myosin II) in *D. discoideum* cells during free migration (A), early stage of cytokinesis (B), and at the completion of cytokinesis (C). In migrating cells, MHCK-C (red dots) colocalizes with myosin II (blue dots) at the posterior region. MHCK-A (green dots), on the other hand, colocalizes with actin at the front protrusions. MHCK-B distributes homogeneously in the cytoplasm (yellow fill). In the early stage of cytokinesis, myosin II concentrates to the furrow. However, MHCK-A (and sometimes MHCK-C) localizes to the polar protrusions (pseudopods) while MHCK-B is always cytosolic throughout the cell with some exclusion from the furrow region. At the late stages of cytokinesis, MHCK-C is recruited to the furrow region, and persists at this location after the completion of division. This persistent localization is reflected as posterior localization in the two new daughter cells, where MHCK-C presumably to help disassemble myosin II thick filaments that have completed their role in furrow contraction.

Materials and Methods
Plasmid construction
The GFP fusions to MHCK A, MHCK B, and MHCK C were constructed by placing GFP at the amino-terminus of each

kinase coding region, with GFP fused to codon 2 of each kinase open reading frame. All fusions were made in the GFP expression vector pTX-GFP [36]. The construct for MHCK A has been described previously [23]. Protein sequences for MHCK A, MHCK B, and MHCK C correspond to GenBank entries A55532, AAB50136, and AAC31918, respectively. Cloning of the cDNA encoding MHCK-C has been described [18].

FLAG-MHCK-C purification and phosphorylation assays
A FLAG epitope was fused to the amino-terminus of MHCK-C at codon 2 using the vector pTX-FLAG [36]. The resulting plasmid, pTX-MKC2, was transformed into the cell line Ax2 and clonal cell lines were selected with G418 (8 μg/ml) in HL-5 medium. To facilitate FLAG-MHCK-C protein purification, Ax2/pTX-MKC2 cell lines were then subjected to incremental increases in G418 selection level over approximately 3 weeks, to a final selection level of 40 μg/ml. As reported previously for expression of MHCK-A [24], this selection process resulted in cell lines with increased expression level of FLAG-MHCK-C, several-fold higher than the initial expression level. In previous work, when this method was applied to MHCK-A-expressing cell lines the elevated expression of MHCK-A resulted in myosin II hyperphosphorylation and myosin II filament disassembly, and corresponding loss of ability of cells to grow in suspension [24]. We observed the same effect in the current studies in attempting to force high expression of FLAG-MHCK-C. The pTX-MKC2 plasmid was therefore transfected into 3xALA myosin II cells, which are resistant to myosin filament hyperphosphorylation and disassembly due to elimination of phosphorylation target sites in the myosin tail [24]. The resultant 3xALA/pTX-MKC2 cells could be propagated in suspension culture even after selection for elevated expression in 40 μg/ml G418.

For purification of FLAG-MHCK-C, 8–10 liters of 3xALA/ pTX-MKC2 cells were propagated in suspension culture in HL-5 medium to approximately 5×10^6 cells/ml. All subsequent steps were performed at 0–4°. Cells were harvested by centrifugation (40–50 g typical yield), then washed once in 50 mM Tris, 150 mM NaCl, pH 7.5 (TBS). Cells were resuspended with 4 ml/g cells in 50 mM Tris pH 8, 1 mM DTT, 1 mM EDTA. Protease inhibitor cocktails PIC1 and PIC2 [22] from a 1000X stock were then added to 5X final concentration, and cells lysed either by sonication or by repeated douncing. Lysate was adjusted to 300 mM NaCl (to dissociate MHCK-C from binding to particulate material), then subjected to centrifugation at $125,000 \times g$ for 20 min. The resulting cleared supernatant was brought to 30% saturation with powdered ammonium sulfate and incubated with stirring for 30 min. The ammonium sulfate precipitate, containing the FLAG-MHCK-C protein, was collected by centrifugation and resuspended with gentle douncing in 20 ml TBS containing 1 mM EDTA

(TBSE), and 1X PIC1 and PIC2. This sample was mixed with 2 ml of anti-FLAG epitope monoclonal antibody-conjugated-beads (M2 beads, Sigma) for 2 hours at 4°. Resin was then washed 3X by centrifugation with 10 ml TBSE and transferred to a small disposable column. Resin was washed with a low concentration of competing FLAG peptide (Sigma; 10 μg/ml in TBSE), then the column was eluted with 2 ml of competing FLAG peptide at 120 μg/ml in TBSE. Eluted protein was concentrated by dialysis against powdered polyethylene glycol (Aquacide; Calbiochem), then dialyzed into 20% glycerol, 20 mM Tris pH 7.5, 20 mM KCl, 1 mM EDTA, 1 mM DTT. This purified FLAG-MHCK C was then aliquoted and stored at -80°C.

Dictyostelium myosin II was purified as described [22]. Phosphorylation reactions with myosin II and FLAG-MHCK-C were performed in 20 mM TES pH 7, 2 mM $MgCl_2$, and 0.5 mM ATP, with ^{32}P-γ-ATP included at 800 Ci/mol final concentration. Peptide phosphorylation assays were done with the peptide MH-1 as substrate at 50 μM. This 16-residue peptide corresponds to the phosphorylation target site at position 2029 of MHC. This peptide and the filter-binding assay used to measure its phosphorylation have been described previously [31]. All peptide phosphorylation studies were performed under conditions in which no more than 30% of the substrate was consumed to ensure linear reaction rates.

Antiserum production
The catalytic domain of MHCK-C was expressed in bacteria and purified using nickel chelation chromatography as described [18]. Purified protein was injected into New Zealand White rabbits at two week intervals for a total of five injections, followed by a terminal bleed. Western blots were performed using total serum at a dilution of 1/2000 and chemiluminscent detection.

GFP-Cell culture
pTX-MKA1, pMKB-GFP, pTX-MKC1 were transformed into either Ax2 cell line [37] or HS1 myosin null cells, a strain of *D. discoideum* with its endogenous *mhc*A gene deleted [38] to generate GFP-MHCK-A, -B, and -C cells, respectively. p102 [34] which encodes GFP-myosin II, was transformed into the HS1 myosin null cells.

Transformations were performed by electroporation [39] and transformed cells were selected by 7.5 μg/ml G418 (Geneticin; Life Technologies, Gaithersburg, MD). *D. discoideum* cells expressing GFP-MHCK's as well as GFP-myosin II-expressing cells were grown and maintained in DdHL-5 media [40] supplemented with 60 μg/ml streptomycin, 60 U/ml penicillin and 7.5 μg/ml G418. Bacterial lawns were prepared by spreading 2 ml of an overnight *Klebsiella aerogenes* culture on SM/5 plates [41].

Fluorescence microscopy
Cells were imaged in a chambered coverslip (Nunc, Naperville, IL) filled with MES buffer (20 mM 2-[morpholino]ethane-sulfonic acid, pH 6.8, 0.2 mM $CaCl_2$, 2 mM $MgSO_4$) at 21°C. Imaging was done as previously described (Sabry et al., 1997) with the following modifications. The light source was replaced to a Xe arc lamp that has 60% increase over the typical input power of an epifluorescent lamp and therefore delivers higher output. This is beneficial when viewing low GFP-expressing cells. For imaging cells reported here, the light was typically attenuated to between 3% to 10% output. The output of the lamp is directed to the microscope by a liquid light-guide. This set up greatly reduces the effect of vibration and heat on the samples and the microscope. Images were collected and analyzed using MetaMorph software (Universal Imaging Corp., West Chester, PA).

Total internal reflection fluorescence microscopy
Using an objective-typed TIRF microscopy, cells were imaged in an anodized aluminum imaging chamber filled with MES buffer (described above) through a coverslip with a refractive index of 1.78. GFP-protein molecules were excited by 488 nm photons produced from an Argon ion laser (Melles Griot) and a 100× (NA = 1.65) objectiv (Olympus). Fluorescent emission was detected through a PentaMax intensified CCD (Princeton Intruments). Typically, each movie collected by Winview (Roper Scientific) was 1 frame/sec for 200 sec, and was subsequently analyzed using NIH image. The apparent length of fluorescent objects was determined using NIH Image (National Institute of Health) to enlarge and identify large (> 10 fold) differences in pixel intensity to identity object edges using the "line-scan" function. Objects that were not clearly separate were removed from consideration."

Authors' contributions
W.L. performed the microscopy imaging, and participated in microscopy design and planning. L.S.L. performed all the biochemical studies and participated in their planning and design. H.M.W. participated in the microscopy imaging, data collection and processing, and experimental planning. J.A.S. and T.T.E. participated in the conception of these studies, in design and coordination, and in data evaluation.

Additional file 1
Time-lapse movie corresponding to figure 5A
Click here for file
[http://www.biomedcentral.com/content/supplementary/1471-2121-3-19-S1.mov]

Additional file 2

Time-lapse movie corresponding to figure 8-M
Click here for file
[http://www.biomedcentral.com/content/supplementary/1471-2121-3-19-S2.mov]

Additional file 3

Time-lapse movie corresponding to figure 8-C1
Click here for file
[http://www.biomedcentral.com/content/supplementary/1471-2121-3-19-S3.mov]

Additional file 4

Time-lapse movie corresponding to figure 8-C2
Click here for file
[http://www.biomedcentral.com/content/supplementary/1471-2121-3-19-S4.mov]

Acknowledgements

References

1. De Lozanne A, Spudich JA: **Disruption of the Dictyostelium myosin heavy chain gene by homologous recombination.** *Science* 1987, **236:**1086-1091
2. Knecht DA, Loomis WF: **Antisense RNA inactivation of myosin heavy chain gene expression in Dictyostelium discoideum.** *Science* 1987, **236:**1081-1086
3. Wessels D, Soll DR, Knecht D, Loomis WF, De Lozanne A, Spudich J: **Cell motility and chemotaxis in Dictyostelium amebae lacking myosin heavy chain.** *Dev Biol* 1988, **128:**164-177
4. Glotzer M: **Animal cell cytokinesis.** *Annu Rev Cell Dev Biol* 2001, **17:**351-386
5. Yumura S: **Myosin II dynamics and cortical flow during contractile ring formation in Dictyostelium cells.** *J Cell Biol* 2001, **154:**137-146
6. Fukui Y, De Lozanne A, Spudich JA: **Structure and function of the cytoskeleton of a Dictyostelium myosin-defective mutant.** *J Cell Biol* 1990, **110:**367-378
7. Sabry JH, Moores SL, Ryan S, Zang JH, Spudich JA: **Myosin Heavy Chain Phosphorylation Sites Regulate Myosin Localization during Cytokinesis in Live Cells.** *Mol Biol Cell* 1997, **8:**2605-2615
8. Weber I, Neujahr R, Du A, Kohler J, Faix J, Gerisch G: **Two-step positioning of a cleavage furrow by cortexillin and myosin II.** *Curr Biol* 2000, **10:**501-506
9. Luck-Vielmetter D, Schleicher M, Grabatin B, Wippler J, Gerisch G: **Replacement of threonine residues by serine and alanine in a phosphorylatable heavy chain fragment of Dictyostelium myosin II.** *FEBS Lett* 1990, **269:**239-243
10. Vaillancourt JP, Lyons C, Côté GP: **Identification of two phosphorylated threonines in the tail region of Dictyostelium myosin II.** *J Biol Chem* 1988, **263:**10082-10087
11. Egelhoff TT, Lee RJ, Spudich JA: **Dictyostelium myosin heavy chain phosphorylation sites regulate myosin filament assembly and localization in vivo.** *Cell* 1993, **75:**363-371
12. Stites J, Wessels D, Uhl A, Egelhoff T, Shutt D, Soll DR: **Phosphorylation of the Dictyostelium myosin II heavy chain is necessary for maintaining cellular polarity and suppressing turning during chemotaxis.** *Cell Motil Cytoskeleton* 1998, **39:**31-51
13. Kuczmarski ER, Spudich JA: **Regulation of myosin self-assembly: phosphorylation of Dictyostelium heavy chain inhibits formation of thick filaments.** *Proc Natl Acad Sci U S A* 1980, **77:**7292-7296
14. Côté GP, Bukiejko U: **Purification and characterization of a myosin heavy chain kinase from Dictyostelium discoideum.** *J Biol Chem* 1987, **262:**1065-1072
15. Côté GP, McCrea SM: **Selective removal of the carboxyl-terminal tail end of the Dictyostelium myosin II heavy chain by chymotrypsin.** *J Biol Chem* 1987, **262:**13033-13038
16. Futey LM, Medley QG, Côté GP, Egelhoff TT: **Structural analysis of myosin heavy chain kinase A from *Dictyostelium*. Evidence for a highly divergent protein kinase domain, an amino-terminal coiled-coil domain, and a domain homologous to the β-subunit of heterotrimeric G proteins.** *J Biol Chem* 1995, **270:**523-529
17. Clancy CE, Mendoza MG, Naismith TV, Kolman MF, Egelhoff TT: **Identification of a Protein Kinase from Dictyostelium with Homology to the Novel Catalytic Domain of Myosin Heavy Chain Kinase A.** *J Biol Chem* 1997, **272:**11812-11815
18. Luo X, Crawley SW, Steimle PA, Egelhoff TT, Côté GP: **Specific phosphorylation of threonine by the dictyostelium myosin ii heavy chain kinase family.** *J Biol Chem* 2001, **276:**17836-17843
19. Ryazanov AG, Pavur KS, Dorovkov MV: **Alpha-kinases: a new class of protein kinases with a novel catalytic domain [letter].** *Curr Biol* 1999, **9:**R43-R45
20. Ryazanov AG, Ward MD, Mendola CE, Pavur KS, Dorovkov MV, Wiedmann M, *et al*: **Identification of a new class of protein kinases represented by eukaryotic elongation factor-2 kinase.** *Proc Natl Acad Sci U S A* 1997, **94:**4884-4889
21. Runnels LW, Yue L, Clapham DE: **TRP-PLIK, a bifunctional protein with kinase and ion channel activities.** *Science* 2001, **291:**1043-1047
22. Steimle PA, Naismith T, Licate L, Egelhoff TT: **WD Repeat Domains Target Dictyostelium Myosin Heavy Chain Kinases by Binding Directly to Myosin Filaments.** *J Biol Chem* 2001, **276:**6853-6860
23. Steimle PA, Yumura S, Côté GP, Medley QG, Polyakov MV, Leppert B, *et al*: **Recruitment of a myosin heavy chain kinase to actin-rich protrusions in Dictyostelium.** *Curr Biol* 2001, **11:**708-713
24. Kolman MF, Egelhoff TT: **Dictyostelium myosin heavy chain kinase A subdomains. Coiled-coil and WD repeat roles in oligomerization and substrate targeting.** *J Biol Chem* 1997, **272:**16904-16910
25. Medley QG, Gariepy J, Côté GP: **Dictyostelium myosin II heavy-chain kinase A is activated by autophosphorylation: studies with Dictyostelium myosin II and synthetic peptides.** *Biochemistry* 1990, **29:**8992-8997
26. Hanakam F, Albrecht R, Eckerskorn C, Matzner M, Gerisch G: **Myristoylated and non-myristoylated forms of the pH sensor protein hisactophilin II: intracellular shuttling to plasma membrane and nucleus monitored in real time by a fusion with green fluorescent protein.** *EMBO J* 1996, **15:**2935-2943
27. Shroeder TE: **The contractile ring and furrowing in dividing cells.** *Ann NY Acad Sci* 1990, **582:**78-87
28. Axelrod D, Hellen EH, Fulbright RM: **Total internal reflection fluorescence.** *In Topics in Fluorescence Spectroscopy: Biochemical Applications. (Edited by: Lakowicz J) New York: Plenum Press* 1992, 289
29. Clarke M, Spudich JA: **Biochemical and structural studies of actomyosin-like proteins from non-muscle cells.** *J Mol Biol* 1974, **86:**209-222
30. Yumura S, Fukui Y: **Reversible cyclic AMP-dependent change in distribution of myosin thick filaments in Dictyostelium.** *Nature* 1985, **314:**194-196
31. Medley QG, Lee SF, Côté GP: **Purification and characterization of myosin II heavy chain kinase A from Dictyostelium.** *Methods Enzymol* 1991, **196:**23-34
32. Medley QG, Bagshaw WL, Truong T, Côté GP: **Dictyostelium myosin II heavy-chain kinase A is activated by heparin, DNA and acidic phospholipids and inhibited by polylysine, polyarginine and histones.** *Biochim Biophys Acta* 1992, **1175:**7-12
33. Bray D, White JG: **Cortical flow in animal cells.** *Science* 1988, **239:**883-888
34. Robinson DN, Cavet G, Warrick HM, Spudich JA: **Quantitation of the Distribution and Flux of Myosin-II during Cytokinesis.** *BMC Cell Biology* 2002, **3:**4
35. Larochelle DA, Epel D: **Myosin Heavy Chain Dephosphorylation During Cytokinesis in Dividing Sea Urchin Embryos.** *Cell Motil* 1993, **25:**369-380

36. Levi S, Polyakov M, Egelhoff TT: **Green Fluorescent Protein and Epitope Tag Fusion Vectors for Dictyostelium discoideum.** *Plasmid* 2000, **44:**231-238

37. Watts DJ, Ashworth JM: **Growth of myxameobae of the cellular slime mould Dictyostelium discoideum in axenic culture.** *Biochem J* 1970, **119:**171-174

38. Ruppel KM, Uyeda TQ, Spudich JA: **Role of highly conserved lysine 130 of myosin motor domain. In vivo and in vitro characterization of site specifically mutated myosin.** *J Biol Chem* 1994, **269:**18773-18780

39. Egelhoff TT, Titus MA, Manstein DJ, Ruppel KM, Spudich JA: **Molecular genetic tools for study of the cytoskeleton in Dictyostelium.** *Methods Enzymol* 1991, **196:**319-334

40. Manstein DJ, Schuster HP, Morandini P, Hunt DM: **Cloning vectors for the production of proteins in Dictyostelium discoideum.** *Gene* 1995, **162:**129-134

41. Sussman M: **Cultivation and synchronous morphogenesis of Dictyostelium under controlled experimental conditions.** *Methods Cell Biol* 1987, **28:**9-29